

Chapter 2

Characterizing Objects and Sensors

In most cases, not all properties characterizing observed objects in a certain application have the same importance for producing a situation picture or can be inferred by the sensor systems involved. At the very beginning, we have to identify suitable object properties relevant to the underlying requirements, which are called *state quantities*. In the context discussed here, state quantities are completely described by numbers or appropriate collections of numbers and may be time-dependent. All relevant properties characterizing an object of interest at a certain instant of time t_k , $k \in \mathbb{N}$, are gathered in a collection X_k of state quantities, which is called *object state* at time t_k . Object states can also be composed of the individual object states of an object group.

2.1 Examples of State Quantities

1. As a first example, consider a vehicle moving on a road approximately modeled by a curve. If the vehicle's position or speed on the road at a time t_k only has interest, the corresponding object state is composed by two real numbers: the arc-length x_k of a point on the curve, representing its position, and its temporal derivative \dot{x}_k , representing its speed. The corresponding object state is thus given by a two-dimensional vector: $X_k = \mathbf{x}_k$ with $\mathbf{x}_k = (x_k, \dot{x}_k)^\top \in \mathbb{R}^2$.
2. Another practically important example is the kinematic state X_k of an object moving in the three-dimensional space at a given instant of time t_k , which is typically given by its position \mathbf{r}_k , velocity $\dot{\mathbf{r}}_k$, and acceleration $\ddot{\mathbf{r}}_k$ at this time. X_k is thus represented by a 9-dimensional vector $X_k = \mathbf{x}_k$ with $\mathbf{x}_k = (\mathbf{r}_k^\top, \dot{\mathbf{r}}_k^\top, \ddot{\mathbf{r}}_k^\top)^\top \in \mathbb{R}^9$.
3. A natural generalization of this concept is the notion of the joint state of two or more objects of interest that form an object group. If kinematic object characteristics are of interest, the corresponding object state X_k is given by a possibly high-dimensional vector $X_k = \mathbf{x}_k$ with $\mathbf{x}_k = (\mathbf{x}_k^{1\top}, \mathbf{x}_k^{2\top}, \dots)^\top$.

4. The notion of object states, however, is broader and includes other characteristic state quantities. In certain applications, object attributes can be described by positive real numbers $x_k \in \mathbb{R}^+$, related to the object's backscattering properties, for example, such as its characteristic mean radar cross section. In this case, a relevant object state may be given by $X_k = (\mathbf{x}_k, x_k)$, where the individual state quantities \mathbf{x}_k (e.g. kinematics) and x_k (e.g. cross section) are taken from different sets of numbers.
5. Stationary or moving objects may belong to distinct classes. Let the object property "object belongs at time t_k to class i_k " be denoted by $i_k \in \mathbb{N}$. Moving objects, for example, can be classified according to the dynamics mode currently in effect, or according to certain characteristic features indicating, e.g., their chemical signatures. Examples of object classes relevant to air surveillance are: *bird, glider, helicopter, sporting airplane, passenger jet, fighter aircraft, missile*. In this case, a characteristic object state is given by $X_k = (\mathbf{x}_k, i_k)$.
6. For describing spatially extended objects or collectively moving object clusters, the kinematic state vector \mathbf{x}_k must be complemented by an additional state quantity characterizing their spatial extension. For the sake of simplicity and to deal with the extended object or cluster tracking problem as rigorously as possible, we confine the discussion to the practically important case of *ellipsoidal* object or cluster extensions. In this case, the current extension at time t_k can be described mathematically by a symmetric and positively definite matrix \mathbf{X}_k . According to this approach, the following object properties are covered:
 - *Size*: volume of the extension ellipsoid
 - *Shape*: ratio of the corresponding semi-axes
 - *Orientation*: direction of the semi-axes.

The corresponding object state is thus given by $X_k = (\mathbf{x}_k, \mathbf{X}_k)$.

Since object states must be inferred from incomplete and imperfect information sources, the collection of state quantities such as

$$X_k = (\mathbf{x}_k, x_k, \mathbf{X}_k, i_k) \quad (2.1)$$

or some of them are interpreted as *random variables*. The application of other, more general notions of uncertainty is possible (see [1], e.g.), but excluded here. According to the Bayesian interpretation of probability theory, all available knowledge on the objects of interest at time t_k is mathematically precisely represented by probability densities of their corresponding states $p(X_k)$. If only one state quantity is of interest, for example in \mathbf{x}_k , $p(\mathbf{x}_k)$ is given by a marginal density:

$$p(\mathbf{x}_k) = \sum_{i_k} \int dx_k d\mathbf{X}_k p(\mathbf{x}_k, x_k, \mathbf{X}_k, i_k). \quad (2.2)$$

Methods to calculate the probability density functions related to object states with at least approximate accuracy is the main goal in Bayesian sensor data fusion.

2.2 Object Evolution Models

Object states usually change in time. Their temporal evolution, however, is imperfectly known in most cases. This fundamental ignorance can often be described by a probability density function of the object state at time t_k , which is conditioned on the previous state X_{k-1} , called transition density $p(X_k|X_{k-1})$, i.e. . With an underlying Markov assumption, knowledge about future object states can be predicted from prior knowledge via the Chapman-Kolmogorov equation:

$$p(X_k) = \int dX_{k-1} p(X_k|X_{k-1}) p(X_{k-1}). \quad (2.3)$$

The temporal evolution described by $p(X_k|X_{k-1})$ mirrors the real object evolution insofar as it allows a Monte-Carlo-simulation of a subsequent state X_k by generating random realizations of it according to the density $p(X_k|X_{k-1})$. It is thus reasonable to call the conditional probability density $p(X_k|X_{k-1})$ the *evolution model* of an object. In the sequel, the notion of an evolution model is illustrated by examples. A wide variety of object evolution models for kinematic object states has been described in the handbook [2, Chap. 1.5] and a series of survey papers [3–7], which are adapted to the particular requirements of the underlying application.

2.2.1 Van-Keuk's Evolution Model

An early and particularly intuitive example of state evolution models in the context of tracking and sensor data fusion was proposed by Günther van Keuk in 1971 [8]. According to van Keuk, the motion of an object is described by a linear equation with additive white Gaussian noise:

$$\mathbf{x}_k = \mathbf{F}_{k|k} \mathbf{x}_{k-1} + \mathbf{G}_{k|k-1} \mathbf{v}_k, \quad (2.4)$$

referring to kinematic object states given by $\mathbf{x}_k = (\mathbf{r}_k^\top, \dot{\mathbf{r}}_k^\top, \ddot{\mathbf{r}}_k^\top)^\top$. The Gaussian random vector \mathbf{v}_k is described by a zero-mean, unit-covariance Gaussian probability density $p(\mathbf{u}_k) = \mathcal{N}(\mathbf{u}_k; \mathbf{0}, \mathbf{1})$. More generally, let a Gaussian be denoted by $\mathcal{N}(\mathbf{x}; \mathbb{E}[\mathbf{x}], \mathbb{C}[\mathbf{x}]) = |2\pi \mathbb{C}[\mathbf{x}]|^{-\frac{1}{2}} \exp\{-\frac{1}{2}(\mathbf{x} - \mathbb{E}[\mathbf{x}])^\top \mathbb{C}[\mathbf{x}]^{-1}(\mathbf{x} - \mathbb{E}[\mathbf{x}])\}$ with an expectation vector $\mathbb{E}[\mathbf{x}]$ and a symmetric, positively definite covariance matrix $\mathbb{C}[\mathbf{x}]$. The matrix $\mathbf{F}_{k|k-1}$ is called *evolution matrix*,

$$\mathbf{F}_{k|k-1} = \begin{pmatrix} \mathbf{1} & (t_k - t_{k-1}) \mathbf{1} & \frac{1}{2}(t_k - t_{k-1})^2 \mathbf{1} \\ \mathbf{0} & \mathbf{1} & (t_k - t_{k-1}) \mathbf{1} \\ \mathbf{0} & \mathbf{0} & e^{-(t_k - t_{k-1})/\theta_t} \mathbf{1} \end{pmatrix} \quad (2.5)$$

with a modeling parameter θ_t , while the matrix $\mathbf{G}_{k|k-1}$ is given by:

$$\mathbf{G}_{k|k-1} = q_t \sqrt{1 - e^{-2(t_k - t_{k-1})/\theta_t}} (\mathbf{O}, \mathbf{O}, \mathbf{1})^\top, \quad (2.6)$$

implying a second modeling parameter q_t . According to this evolution model, straightforward calculations show that the acceleration $\ddot{\mathbf{r}}_k$ is described by an ergodic, zero-mean Gauß-Markov process with an autocorrelation function given by:

$$\mathbb{E}[\ddot{\mathbf{r}}_k \ddot{\mathbf{r}}_l^\top] = q_t^2 \exp[-(t_k - t_l)/\theta_t] \mathbf{1}, \quad l \leq k. \quad (2.7)$$

This expression clearly defines the modeling parameters q_t (*acceleration bandwidth*) and θ_t (*maneuver correlation time*), which have characteristic values for different classes of maneuvering objects. The corresponding Gauß-Markov transition density is given by:

$$p(\mathbf{x}_k | \mathbf{x}_{k-1}) = \mathcal{N}(\mathbf{x}_k; \mathbf{F}_{k|k-1} \mathbf{x}_{k-1}, \mathbf{D}_{k|k-1}) \quad (2.8)$$

where $\mathbf{D}_{k|k-1} = \mathbf{G}_{k|k-1} \mathbf{G}_{k|k-1}^\top$ is called *evolution covariance matrix*.

2.2.2 Interacting Multiple Models

In practical applications, it might be uncertain which evolution model out of a set of r possible alternatives is currently in effect. In the case of air targets, for example, we can distinguish between different flight phases (no turn, slight maneuver, high-g, turn etc.). According to the previous discussion, the maneuvering class $1 \leq i_k \leq r$, to which an object belongs at time t_k , can be considered as a part of its state. In general, Markovian evolution models for object states $X_k = (\mathbf{x}_k, i_k)$ are expressed by:

$$p(x_k, i_k | x_{k-1}, i_{k-1}) = p(x_k | i_k, x_{k-1}, i_{k-1}) p(i_k | x_{k-1}, i_{k-1}). \quad (2.9)$$

A special case that implies additional assumptions is defined by:

$$p(x_k, i_k | x_{k-1}, i_{k-1}) = p(x_k | i_k, x_{k-1}) p(i_k | i_{k-1}) \quad (2.10)$$

$$= p_{i_k i_{k-1}} \mathcal{N}(\mathbf{x}_k; \mathbf{F}_{k|k-1}^{i_k} \mathbf{x}_{k-1}, \mathbf{D}_{k|k-1}^{i_k}) \quad (2.11)$$

and is called *IMM evolution model* (IMM: Interaction Multiple Models, see [7] and the literature cited therein) and has been introduced by HENK BLOM [9]. IMM models are characterized by r purely kinematic transition densities $p(\mathbf{x}_k | \mathbf{x}_{k-1}, i_k)$, for instance of the van Keuk type, and class transition probabilities $p_{i_k i_{k-1}} = p(i_k | i_{k-1})$ that must be specified and are part of the modeling assumptions. The transition probabilities $p_{i_k i_{k-1}}$ define a stochastic matrix. According to $\sum_{i_k=1}^r p(i_k | i_{k-1}) = 1$ the columns of such matrices must add up to one.

Note that Eq. 2.11 assumes that $p(x_k | x_{k-1}, i_k, i_{k-1})$ is independent of the past maneuvering class i_{k-1} and $p(i_k | \mathbf{x}_{k-1}, i_{k-1})$ does not depend on the object's kinematic state \mathbf{x}_{k-1} . While the first assumption seems to be quite natural, the second

may be an oversimplification in certain cases. As an example, let us consider two evolution models describing low and strong maneuvers, respectively. The probability $p(i_k = 1|i_k = 1, \mathbf{x}_{k-1})$ that an object stays in the low maneuver model increases as the object acceleration diminishes, while $p(i_k = 2|i_k = 2, \mathbf{x}_{k-1})$ increases as the acceleration increases. If q is a measure of the maximum acceleration, state-dependent transition matrices of the form

$$\begin{pmatrix} p_{11}e^{-\frac{1}{2}\frac{|\dot{\mathbf{r}}_k|^2}{q^2}} & 1 - p_{22}(1 - e^{-\frac{1}{2}\frac{|\dot{\mathbf{r}}_k|^2}{q^2}}) \\ 1 - p_{11}e^{-\frac{1}{2}\frac{|\dot{\mathbf{r}}_k|^2}{q^2}} & p_{22}(1 - e^{-\frac{1}{2}\frac{|\dot{\mathbf{r}}_k|^2}{q^2}}) \end{pmatrix} \quad (2.12)$$

can model this type of object behavior [10]. For $r = 1$, the linear-Gauß-Markov models result as a limiting case.

2.3 Sensor Likelihood Functions

Over time, one or several sensors produce sets of measurement data Z_k that potentially carry information on object states X_k characterizing one or more objects of interest at time t_k . This information is typically imprecise and corrupted by unavoidable measurement errors, e.g. In several applications, a sensor output Z_k can refer to individual properties of several neighboring objects of interest, but it is usually unknown to which particular object. In addition, some or all sensor data can be false, i.e. be originated by unwanted objects or unrelated to really existing objects. It is furthermore not necessarily true that sensors always produce measurements of objects of interest when an attempt is made. Moreover, several closely-spaced objects may produce irresolved measurements originated by two or more objects.

At discrete instants of time t_k , we consider the set $Z_k = \{Z_k^j\}_{j=1}^{m_k}$ of m_k sensor data. The accumulation of the sensor data Z_l , $1 \leq l \leq k$, up to and including the time t_k , typically the present, is an example of a time series recursively defined by $Z^k = \{Z_k, m_k, Z^{k-1}\}$. The time series produced by the measurements of individual sensors s involved are denoted by $Z_s^k = \{Z_l^s, m_l^s\}_{l=1}^k$, $1 \leq s \leq S$.

Within the framework of Bayesian reasoning, imperfect knowledge about what measured sensor data Z_k can actually say about the states of the objects involved is modeled by interpreting Z_k as a set of random variables. The statistical properties of Z_k are characterized by a probability density function $p(Z_k|X_k)$, which is conditioned on the corresponding object state X_k referring to the same time t_k . The probability densities $p(Z_k|X_k)$ are also called *likelihood functions* when considered as functions of the random variable X_k for a given sensor output Z_k . Typically, likelihood functions need to be known only up to a factor independent of X_k ,

$$\ell(X_k; Z_k) \propto p(Z_k|X_k), \quad (2.13)$$

as will become clear below. The sensor data Z_k explicitly enter into the likelihood function, while all sensor properties describing the sensors' physical and technical characteristics and their measurement performance are implicitly part of it and shape its concrete functional form. In particular, all relevant sensor parameters, such as measurement accuracy, detection probability, false alarm density, sensor resolution, minimum detectable velocity, radar beam width, pulse repetition frequency etc., must be present in the likelihood function. A likelihood function thus describes what information on an object state X_k is provided by the sensor data Z_k at a given instant of time t_k . For physical reasons, often $p(Z_k|X_l, Y) = p(Z_k|X_k)$ holds for any other random variable Y that is not part of the object state.

Likelihood functions $p(Z_k|X_k)$ model the real sensor output (and thus the physics of the underlying measurement process and its interaction with the object environment). For this reason, they provide the basis for Monte-Carlo-simulations of the sensor measurements by generating random realizations of Z_k according to $p(Z_k|X_k)$. For this reason, likelihood functions are simply called "sensor models" in direct analogy to "evolution models" given by $p(X_k|X_{k-1})$. Obviously, a sensor model is more correct, the more it provides simulated measurements that correspond on average to the real sensor output.

In the sequel, the notion of a likelihood function is illustrated by selected examples.

2.3.1 Gaussian Likelihood Functions

For well-separated objects, perfect detection, and in absence of false sensor data, let us consider measurements \mathbf{z}_k related to the kinematic state vector $\mathbf{x}_k = (\mathbf{r}_k^\top, \dot{\mathbf{r}}_k^\top, \ddot{\mathbf{r}}_k^\top)^\top$ of an object at time t_k . In constructing a sensor model $p(\mathbf{z}_k|\mathbf{x}_k)$, two questions must be answered:

1. The first question aims at what aspect of the state vector is currently in the focus of the sensor, i.e. at the identification of a *measurement function*,

$$\mathbf{h}_k : \mathbf{x}_k \mapsto \mathbf{h}_k(\mathbf{x}_k), \quad (2.14)$$

describing what is actually measured. Sensors characterized by the same measurement function \mathbf{h}_k are called *homogeneous sensors*, in contrast to *heterogeneous sensors*, where this is not the case.

2. The second question asks for the quality of such a measurement. In many applications, additive measurement errors \mathbf{u}_k can be considered, given by bias-free and Gaussian distributed random variables characterized by a *measurement error covariance matrix* \mathbf{R}_k . The measurement errors produced at different times or by different sensors can usually be considered as independent of each other.

In this case, the measurement process can be described by a *measurement equation* $\mathbf{z}_k = \mathbf{h}_k(\mathbf{x}_k) + \mathbf{v}_k$, which is equivalent to a Gaussian likelihood function:

$$\ell(\mathbf{x}_k; \mathbf{z}_k) = \mathcal{N}(\mathbf{z}_k; \mathbf{h}_k(\mathbf{x}_k), \mathbf{R}_k). \quad (2.15)$$

Range-Azimuth Measurements

In a two-dimensional plane, we may, for example, consider measurements of an object's range r_k and azimuth angle φ_k with respect to the sensor position in a given Cartesian coordinate system. Let the range and azimuth measurements be independent of each other with Gaussian measurement errors described by the standard deviations σ_r, σ_φ . Hence, in polar coordinates, the measurement error covariance matrix is diagonal: $\text{diag}[\sigma_r^2, \sigma_\varphi^2]$. A transformation of the original measurements into the Cartesian coordinate system, where the state vectors \mathbf{x}_k are formulated, is provided by the transform $\mathbf{t}(r_k, \varphi_k) = r_k(\cos \varphi_k, \sin \varphi_k)^\top$. A well-known result on affine transforms of Gaussian random variables (see Appendix A.3) is applicable, if the non-linear function $\mathbf{t}(r_k, \varphi_k)$ is expanded in a Taylor series up to the first order. The corresponding Jacobian can be written as the product of a rotation matrix \mathbf{D}_{φ_k} by φ_k and a dilation matrix \mathbf{S}_{r_k} defined by r_k :

$$\mathbf{T}_k = \frac{\partial \mathbf{t}(r_k, \varphi_k)}{\partial (r_k, \varphi_k)} \quad (2.16)$$

$$= \underbrace{\begin{pmatrix} \cos \varphi_k & -\sin \varphi_k \\ \sin \varphi_k & \cos \varphi_k \end{pmatrix}}_{\text{rotation } \mathbf{D}_{\varphi_k}} \underbrace{\begin{pmatrix} 1 & 0 \\ 0 & r_k \end{pmatrix}}_{\text{dilation } \mathbf{S}_{r_k}}. \quad (2.17)$$

The transformed measurements $\mathbf{z}_k = \mathbf{t}(r_k, \varphi_k)$ can thus be approximately characterized as Gaussian random variables with measurement error covariance matrices \mathbf{R}_k given by:

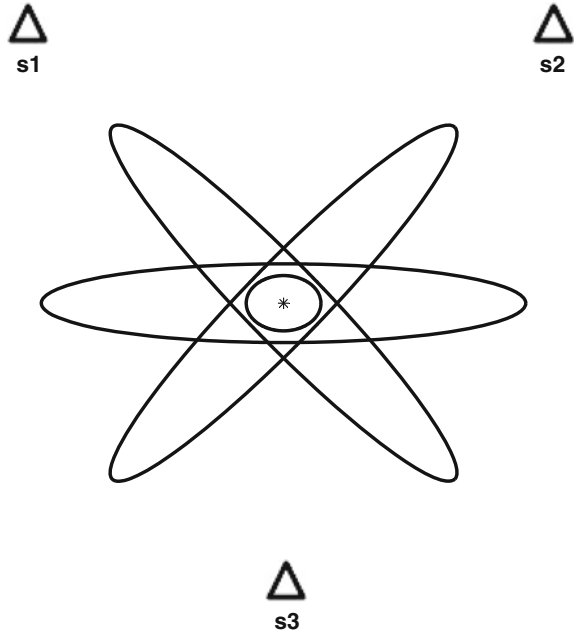
$$\mathbf{R}_k = \mathbf{D}_{\varphi_k} \begin{pmatrix} \sigma_r^2 & 0 \\ 0 & r_k^2 \sigma_\varphi^2 \end{pmatrix} \mathbf{D}_{\varphi_k}^\top. \quad (2.18)$$

according to Eq. A.20. Obviously, the measurement error covariance matrix \mathbf{R}_k depends on the underlying sensor-to-object geometry, i.e. differently located sensors with the same parameters σ_r, σ_φ produce measurements of the same object that are characterized by differently oriented measurement error ellipses as illustrated in Fig. 2.1. The cross-range semi-axis of the measurement error ellipses increases with increasing range, while the other semi-axis remains constant. The orientation of the measurement ellipse depends on the object's azimuth angle φ_k . With a matrix $\mathbf{H}_k = (\mathbf{1}, \mathbf{0}, \mathbf{0})$ that projects the position vector from the object state vector, $\mathbf{H}_k \mathbf{x}_k = \mathbf{r}_k$, the resulting likelihood function is thus given by:

$$\ell(\mathbf{x}_k; \mathbf{z}_k) \propto \mathcal{N}(\mathbf{z}_k; \mathbf{H}_k \mathbf{x}_k, \mathbf{R}_k). \quad (2.19)$$

For a discussion of problems and improvements, e.g. “Unbiased Converted Measurements”, see [2, Chap. 1.7]. In many other applications, we are analogously looking for

Fig. 2.1 Schematic representation of the approximate measurement error ellipses of three sensors located at s_1, s_2, s_3 measuring range and azimuth of an object at $*$ and the impact of the sensor-to-object geometry on their mutual orientation, basic for the geometric fusion gain



formulations where a non-linear measurement function \mathbf{h}_k is linearly approximated by a *measurement matrix* \mathbf{H}_k , possibly depending on time.

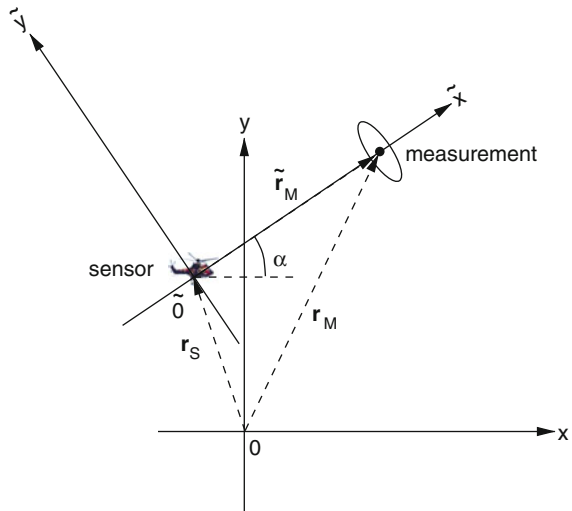
Doppler Measurements

By exploiting the Doppler effect, sensors that receive electromagnetic or acoustic wave forms reflected or emitted by objects of interest, such as radar, sonar, or ultrasonic devices, can measure the radial component \dot{r}_k of an object's relative velocity $\dot{\mathbf{r}}_k - \dot{\mathbf{p}}_k$ with respect to the sensor, where $\dot{\mathbf{p}}_k$ denotes the velocity vector of the sensor platform (see Fig. 2.2). Such frequency-based measurements are often highly precise and important in certain applications such as threat evaluation. The measurement triple $(r_k, \varphi_k, \dot{r}_k)$, however, cannot be transformed into Cartesian coordinates in analogy to the previous considerations. With $(\mathbf{r}_k - \mathbf{p}_k)/|\mathbf{r}_k - \mathbf{p}_k|$, the unit vector pointing from the sensor platform at the position \mathbf{p}_k to the object located at \mathbf{r}_k , the measurement function for range-rate measurements r_k is non-linear and given by:

$$h : \mathbf{x}_k \mapsto h(\mathbf{x}_k; \mathbf{p}_k, \dot{\mathbf{p}}_k) = \frac{(\dot{\mathbf{r}}_k - \dot{\mathbf{p}}_k)^\top (\mathbf{r}_k - \mathbf{p}_k)}{|(\dot{\mathbf{r}}_k - \dot{\mathbf{p}}_k)^\top (\mathbf{r}_k - \mathbf{p}_k)|}. \quad (2.20)$$

Note that in a practical realization sufficiently accurate navigation systems are required to estimate the platform state vector. As mentioned before, an expression following Eq. 2.19 can be obtained by a first-order Taylor expansion of the measurement function.

Fig. 2.2 Transformation of underlying Cartesian coordinates into a measurement-adapted system by a translation and rotation defined by the object's azimuth. Note that the \tilde{x} -axis points towards the object: r_k is thus a measurement of \tilde{x}



This type of non-linear measurement functions, however, can be handled alternatively. Consider a transformation of the underlying coordinates into a Cartesian system, where the origin is at the sensor location, while one of the axes points in a direction defined by the angular measurements (Fig. 2.2). Obviously, this transformation is simply a translation followed by a rotation. In the new coordinate system, the range-rate measurement can be interpreted as a measurement of one of the Cartesian components of the relative velocity vector of the object [11]. This means that the likelihood has a form as in Eq. 2.19 with a linear measurement equation. If a processing scheme is to be applied that requires likelihood functions of this form, a coordinate transform is therefore necessary at each processing step. In this context, Eq. A.20 is relevant, stating that a Gaussian density remains a Gaussian after this transformation. Similar considerations apply if measurements of the radial or lateral object extension is considered [12].

Evaluations with real data show that this type of dealing with range-rate measurements is significantly more robust than approaches based on Taylor expansions. The example leads to the more general observation that the appropriate formulation of sensor models requires a careful study of the individual physical quantity to be measured, quantitative performance evaluations, and comparisons with alternatives in order to achieve efficient and robust sensor models, the basic elements of sensor data fusion systems.

TDoA and FDoA Measurements

In a plane, let the kinematic state of an object emitting electromagnetic signals at time t_k be given by $\mathbf{x}_k = (\mathbf{r}_k^\top, \dot{\mathbf{r}}_k^\top)^\top$. The emitter is observed by $S = 2$ sensors on possibly moving platforms with known state vectors $(\mathbf{p}_k^{s\top}, \dot{\mathbf{p}}_k^{s\top})^\top$, $s = 1, 2$ that passively receive the emitted radiation. The *Time of Arrival (ToA)*, the time interval

from transmitting a signal at the emitter position \mathbf{r}_k and receiving it at a sensor position \mathbf{p}_k^s , is equal to the time the signal needs to travel from the emitter to the sensor. Since we know the propagation speed of the signal (speed of light c), ToA is given by $|\mathbf{r}_k - \mathbf{p}_k^s|/c$. A sensor model for *Time Difference of Arrival (TDoA)* measurements z_k^t directly follows:

$$\ell_t(\mathbf{x}_k; z_k^t) = \mathcal{N}(z_k^t c; h_t(\mathbf{x}_k), \sigma_t/c) \quad (2.21)$$

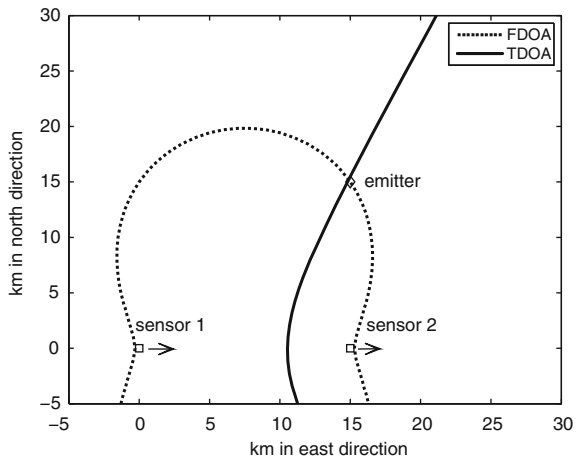
with a measurement function h_t given by:

$$h_t(\mathbf{x}_k; \mathbf{p}_k^1, \mathbf{p}_k^2) = |\mathbf{r}_k - \mathbf{p}_k^1| - |\mathbf{r}_k - \mathbf{p}_k^2|, \quad (2.22)$$

where σ_t denotes the standard deviation of the corresponding TDoA measurement errors. The locations of the sensor platforms enter as parameters. The sign of an individual measurement indicates which of the sensors is closer to the emitter. Without loss of generality, we can thus limit the discussion to one of these cases. The solid line in Fig. 2.3, a hyperbola, shows all potential emitter positions producing the same TDoA measurements, i.e. having the same distance difference from the sensors.

The Doppler shift in frequency is proportional to the radial velocity component of an emitter moving with respect to a Cartesian sensor coordinate system. The inverse wave length λ of the emitted radiation is the proportionality constant. Let $(\mathbf{r}_k - \mathbf{p}_k^s)/|\mathbf{r}_k - \mathbf{p}_k^s|$ denote the unit vector pointing from the sensor position \mathbf{p}_k^s at time t_k to the emitter located at \mathbf{r}_k , moving with the velocity $\dot{\mathbf{r}}_k$. As before, the radial component of the relative velocity of the emitter with respect to the sensor s is given by $(\dot{\mathbf{r}}_k - \dot{\mathbf{p}}_k^s)^\top (\mathbf{r}_k - \mathbf{p}_k^s)/|\mathbf{r}_k - \mathbf{p}_k^s|$. The measurement function for *Frequency Difference of Arrival (FDoA)* measurements is thus given by:

Fig. 2.3 Localization of an emitter using TDoA and FDoA measurements by two moving sensors: constant TDoA/FDoA emitter location curve



$$h_f(\mathbf{x}_k) = \frac{(\dot{\mathbf{r}}_k - \dot{\mathbf{p}}_k^1)^\top (\mathbf{r}_k - \mathbf{p}_k^1)}{|\mathbf{r}_k - \mathbf{p}_k^1|} - \frac{(\dot{\mathbf{r}}_k - \dot{\mathbf{p}}_k^2)^\top (\mathbf{r}_k - \mathbf{p}_k^2)}{|\mathbf{r}_k - \mathbf{p}_k^2|}. \quad (2.23)$$

A constant FDoA curve for a non-moving emitter is shown by the dashed curve in Fig. 2.3, where the arrows indicate the direction of the platform velocities. In this example, TDoA and FDoA are complementary in that TDoA takes the (approximate) role of bearings measurement, and FDoA, the (approximate) role of distance measurement. TDoA and FDoA measurements may be obtained simultaneously by calculating the Complex Ambiguity Function (CAF, [13]), which cross-correlates the signals received by the sensors. The likelihood functions that result from the measurement functions h_t and h_f are shown in Fig. 2.4. Techniques discussed in [14] and applied to emitter localization and tracking, make it possible to approximate the likelihood functions by sums of appropriately chosen individual Gaussians with a linear approximation of the measurement function according to Eq. 2.19.

2.3.2 Multiple Sensor Likelihood

Assume S homogeneous sensors are located at different positions that measure, at the same instant of time t_k , the same linear function $\mathbf{H}_k \mathbf{x}_k$ of an individual kinematic object state \mathbf{x}_k . Under conditions as considered before, let the individual likelihood functions of the sensors be given by:

$$\ell_s(\mathbf{x}_k; \mathbf{z}_k^s) \propto \mathcal{N}(\mathbf{z}_k^s; \mathbf{H}_k \mathbf{x}_k, \mathbf{R}_k^s), \quad s = 1, \dots, S. \quad (2.24)$$

Since independently working sensors were assumed, the over-all likelihood function describing the information on an object state, which is provided by all sensors at time t_k , can be written as a product of the individual likelihood functions:

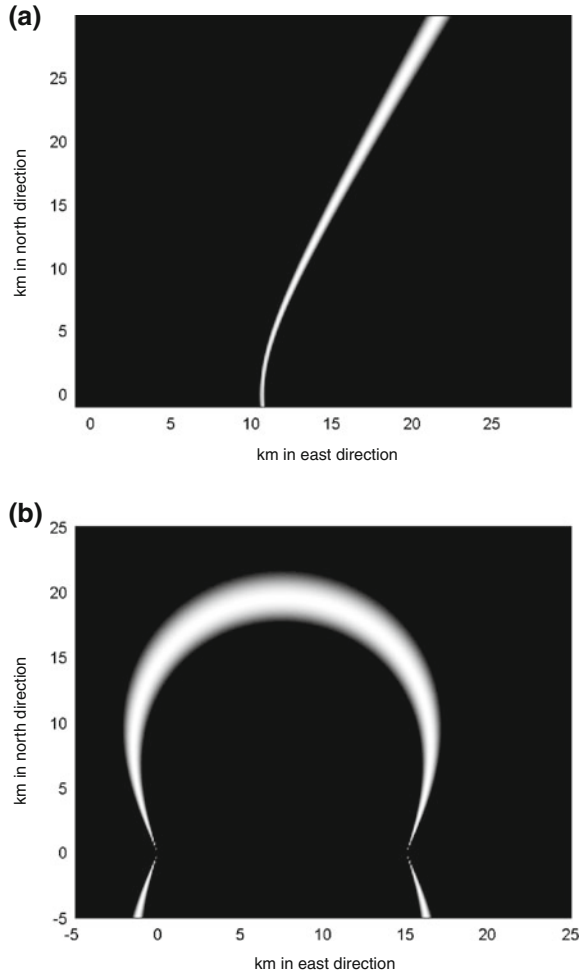
$$\ell(\mathbf{x}_k; \mathbf{z}_k^1, \dots, \mathbf{z}_k^S) \propto \prod_{s=1}^S \mathcal{N}(\mathbf{z}_k^s; \mathbf{H}_k \mathbf{x}_k, \mathbf{R}_k^s). \quad (2.25)$$

In Appendix A.5, a product formula for Gaussians is proven, which is well-suited for simplification of the product representation of the over-all likelihood function. An induction argument directly yields that $\ell(\mathbf{x}_k; \mathbf{z}_k^1, \dots, \mathbf{z}_k^S)$ can be represented by a single Gaussian,

$$\ell(\mathbf{x}_k; \mathbf{z}_k^1, \dots, \mathbf{z}_k^S) \propto \mathcal{N}(\mathbf{z}_k; \mathbf{H}_k \mathbf{x}_k, \mathbf{R}_k) \quad (2.26)$$

with an *effective measurement* \mathbf{z}_k and a corresponding *effective measurement error covariance* \mathbf{R}_k defined by:

Fig. 2.4 Likelihood functions for TDoA and FDoA measurements. Idea: approximate the likelihood functions by a sum of appropriately chosen Gaussians with a linear approximation of the measurement function. **a** Likelihood of TDoA and FDoA measurements. **b** Likelihood of FDoA measurements.



$$\mathbf{R}_k = \left(\sum_{s=1}^S \mathbf{R}_k^{s-1} \right)^{-1} \quad (2.27)$$

$$\mathbf{z}_k = \mathbf{R}_k \sum_{s=1}^S \mathbf{R}_k^{s-1} \mathbf{z}_k^s. \quad (2.28)$$

The effective measurement is thus represented by a *weighted arithmetic mean* of the measurements \mathbf{z}_k^s provided by the individual sensors involved, where the corresponding matrix-valued weighting factors are given by the inverses of the corresponding measurement error covariance matrices \mathbf{R}_k^{s-1} . Obviously, “poor” measurements, characterized by large measurement errors, provide smaller contributions to the effec-

tive measurement \mathbf{z}_k than “good” ones. Dealing with data from multiple sensors in this way is an example of centralized or distributed *measurement fusion* as opposed to *track-to-track fusion* (see the discussion in Sect. 3.1.1). Figure 2.1 illustrates the *geometric fusion gain* \mathbf{R}_k according to Eq. 2.27.

Geometric Fusion Gain

From these considerations several conclusions can be drawn:

1. If all individual measurement covariance matrices are identical, $\mathbf{R}_k^s = \mathbf{R}_k'$, $s = 1, \dots, S$, the effective measurement is the simple arithmetic mean of the individual measurements: $\mathbf{z}_k = \frac{1}{S} \sum_s \mathbf{z}_k^s$. For the effective measurement error covariance, we obtain the ‘square-root’ law: $\mathbf{R}_k = \frac{1}{S} \mathbf{R}_k'$.
2. If all measurement error ellipses involved differ significantly in their geometrical orientation relative to each other, a much greater effect can be observed (geometrical fusion gain).
3. The ‘intersection’ of error ellipses is obtained by calculating the *harmonic mean* of the related error covariance matrices. The harmonic mean of error covariances quantitatively describes the gain by fusing sensor data from several sources and has been referred to as the *Fusion Equation*.
4. In the limiting case of very narrow measurement error ellipses, such as those characterized by $\sigma_r \gg r_k \sigma_\varphi$, the triangulation of an object’s position from bearings only is obtained. Analogously, range-only measurements can be used (trilateration).

These considerations are also valid in three spatial dimensions as well as in more sophisticated sensor data, such as bistatic range or range-rate measurements (see for example [15, 16]).

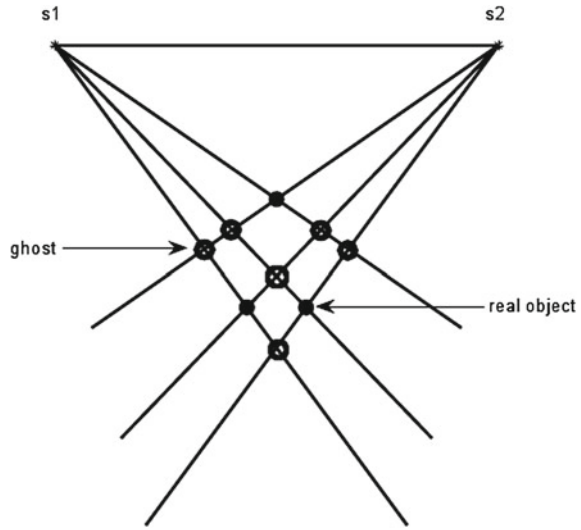
If there is more than one object in the common field of view of bearing-only sensors, not every intersection of two bearings actually corresponds to a real object position. Figure 2.5 illustrates this situation as well as the appearance of *ghosts* that do not correspond to real objects. Of course, in the case of inaccurate, false, missing, or even unresolved bearings, the *de-ghosting* is by no means trivial. For more details and possible solutions of de-ghosting problems in certain applications, see for example [17] (bearing-only tracking) or [18] (passive radar).

Cumulative Detection

In applications with relatively large data innovation intervals between successive data collections, such as in air-to-ground wide-area surveillance, sensor data fusion is particularly important for enhancing the data rate. Assuming measurement fusion as before, we consider the *mean cumulative data innovation intervals* ΔT_c [19] resulting from the individual innovation intervals ΔT_s , $s = 1, \dots, S$ of S sensors, which is defined by:

$$\frac{1}{\Delta T_c} = \sum_{s=1}^S \frac{1}{\Delta T_s}. \quad (2.29)$$

Fig. 2.5 Two objects observed by two bearings-only sensors s_1, s_2 . Not all intersections of bearing correspond to real objects. Typically, the number of “ghosts” is much higher than the number of objects involved



The *cumulative detection probability* is given by $P_D^S = 1 - \prod_{s=1}^S (1 - P_D^s)$, where P_D^s denotes the individual detection probability of sensor s , possibly depending on the corresponding sensor-to-object geometry (see the discussion in Sect. 3.1.2). It is appropriate to introduce the notion of the *mean cumulative detection probability* P_D^C , referring to ΔT_c and defined by:

$$P_D^C = 1 - \prod_{s=1}^S (1 - P_D^s)^{\frac{\Delta T_c}{\Delta T_s}}. \quad (2.30)$$

The data innovation intervals ΔT_s also enter into this formula, which describes the mean improvement of the overall detection performance to be expected by sensor data fusion. The larger ΔT_s , the smaller is the effect of sensor s on the overall performance, even if the corresponding individual detection probability P_D^s is large.

2.3.3 Likelihood for Ambiguous Data

A sensor output at time t_k , consisting of m_k measurements collected in the set Z_k , can be ambiguous, i.e. the origin of the sensor data has to be explained by a set of data interpretations, which are assumed to be exhaustive and mutually exclusive. As an example, let us consider measurements $Z_k = \{\mathbf{z}_k^j\}_{j=1}^{m_k}$ possibly related to the kinematic state \mathbf{x}_k of well-separated objects. ‘Well-separated’ here means that measurements potentially originated by one object could not have been originated by another. Even in this simplified situation, ambiguity can arise from imperfect

detection, false measurements, often referred to as *clutter*, or measurements from unwanted objects.

Illustration

As a schematic illustration of a more general case, let us consider six measurements produced by two closely-spaced objects (see Fig. 2.6). Among other data interpretations, the black dots indicate two measurements assumed as real, while all other data are assumed to be false (Fig. 2.6a). The asterisks denote predicted measurements provided by the tracking system. Under assumptions discussed in (Sect. 3.2.2), object measurements are Gaussian distributed about the predicted measurements with a covariance matrix $\mathbf{S}_{k|k-1}$ determined by the ignorance on the object state as well as by the sensor and the evolution model. The difference vector $\mathbf{v}_{k|k-1}$ between an actual and a predicted measurement is called *innovation*. As will become clear below, the statistical properties of the innovation related to a particular interpretation hypothesis are essential to evaluating its statistical weight. *Gating* means that only those sensor data are considered whose innovations are smaller than a certain predefined threshold in the sense of a Mahalanobis norm: $\mathbf{v}_{k|k-1}^\top \mathbf{S}_{k|k-1}^{-1} \mathbf{v}_{k|k-1} < \chi^2(P_c)$. Expectation gates thus contain the measurements with a given (high) *correlation probability* P_c . Obviously, the ambiguities involved with the situation in Fig. 2.6 are not completely resolved by gating.

More feasible hypotheses, however, compete with the data interpretation previously discussed. For instance, the targets could have produced a single unresolved measurement as indicated in Fig. 2.6b, all other data being false. Alternatively, one of the objects may not have been detected or no detection may have occurred at all. The expectation gates and therefore the ambiguity of the received sensor data grow larger according to an increasing number of false measurements and missed detections as well as to large measurement errors, data innovation intervals, or expected object maneuvers.

Well-separated Objects

Let $j_k = 0$ denote the data interpretation hypothesis that the object has not been detected at all by the sensor at time t_k , i.e. all sensor data have to be considered as false measurements, while $1 \leq j_k \leq m_k$ represents the hypothesis that the object has been detected, $\mathbf{z}_k^{j_k} \in Z_k$ being the corresponding measurement of the object properties, the remaining sensor data being false. Obviously, $\{0, \dots, m_k\}$ denotes a set of mutually exclusive and exhaustive data interpretations.

Due to the total probability theorem and with D or $\neg D$ denoting that the object has or has not been detected, the conditional probability density $p(Z_k, m_k | \mathbf{x}_k)$ can be written as a weighted sum of conditional likelihood functions:

$$p(Z_k, m_k | \mathbf{x}_k) = p(Z_k, m_k, \neg D | \mathbf{x}_k) + p(Z_k, m_k, D | \mathbf{x}_k) \quad (2.31)$$

$$= p(Z_k, m_k | \neg D, \mathbf{x}_k) p(\neg D | \mathbf{x}_k) + p(Z_k, m_k | D, \mathbf{x}_k) p(D | \mathbf{x}_k). \quad (2.32)$$

The sensor model $p(Z_k, m_k | \mathbf{x}_k)$ can be traced back to intuitively understandable physical/technical phenomena and related sensor parameters. As a first consequence,

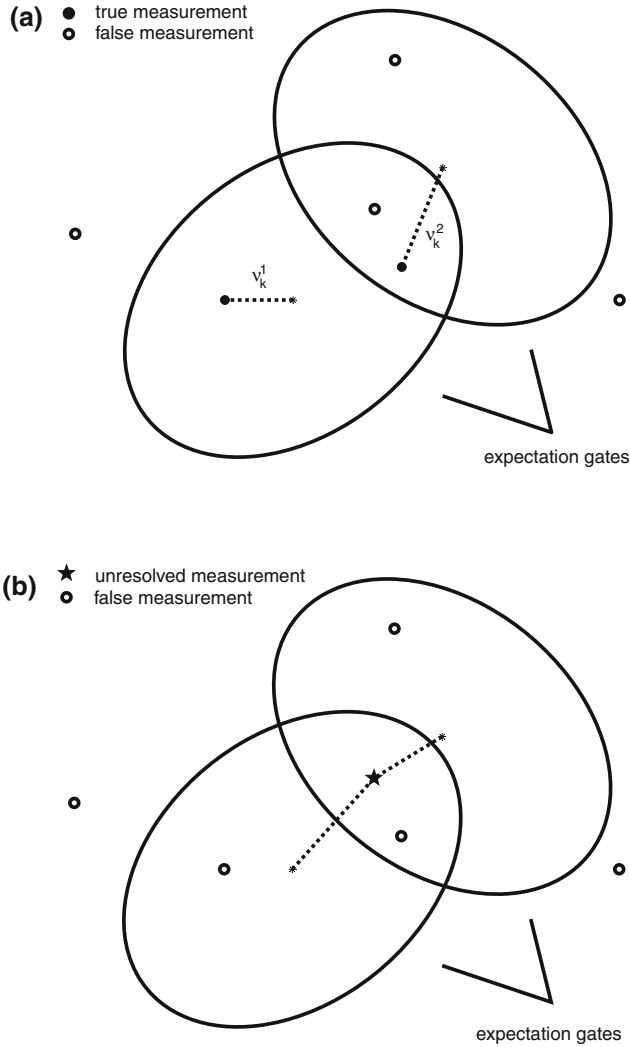


Fig. 2.6 Sensor measurements produced by two closely-spaced objects: competing data interpretations due to uncertain origin of the the sensor data including hypotheses assuming possibly unresolved measurements. **a** Two resolved targets. **b** Two irresolved targets

the *probability of detection*, $p(D|\mathbf{x}_k) =: P_D$, and non-detection, $p(\neg D|\mathbf{x}_k) = 1 - P_D$ enter into the likelihood as a characteristic parameter related to the detection process performed within a sensor system. For the sake of simplicity, we do not express by our notation here that detection probabilities may depend on the object state vectors \mathbf{x}_k . State-dependent detection probabilities, however, become relevant in several real-world applications (see the discussion in Sect. 3.1.2).

1. The conditional likelihood $p(Z_k, m_k | \neg D, \mathbf{x}_k)$ in Eq. 2.32 can be rewritten as:

$$p(Z_k, m_k | \neg D, \mathbf{x}_k) = p(Z_k | m_k, \neg D, \mathbf{x}_k) p(m_k | \neg D, \mathbf{x}_k) \quad (2.33)$$

$$= p_F(m_k) |\text{FoV}|^{-m_k}. \quad (2.34)$$

Here, the probability of having received m_k false measurements given the object was not detected, $p(m_k | \neg D, \mathbf{x}_k)$, is provided by a further modeling assumption, which relates the fluctuating number of false measurements to a mean *spatial clutter density* ρ_F characteristic of the sensor's detection process and the sensing environment. According to modeling assumptions, which are well-proven in many practical applications, let the probability of the number of false data involved $p(m_k | \neg D, \mathbf{x}_k)$ be given by a Poisson distribution

$$p_F(m_k) = (\bar{m}_F^{m_k} / m_k!) e^{-\bar{m}_F} \quad (2.35)$$

with a mean number of false measurements \bar{m}_F , which is related to the volume of the sensor's field of view $|\text{FoV}|$ and ρ_F via $\bar{m}_F = \rho_F |\text{FoV}|$. ρ_F may vary on a larger scale than the direct object neighborhood. Values for ρ_F can either be taken from so-called 'clutter maps', i.e. from related context information, or adaptively be estimated on-line [20–22]. Since false measurements are assumed to be independent from each other and equally distributed in the sensor's field of view (FoV), we have $p(Z_k | m_k, \neg D, \mathbf{x}_k) = \prod_{j=1}^{m_k} p(\mathbf{z}_k^j | \neg D, \mathbf{x}_k) = |\text{FoV}|^{-m_k}$.

2. For the conditional likelihood $p(Z_k, m_k | D, \mathbf{x}_k)$ in Eq. 2.32, we obtain analogously:

$$p(Z_k | m_k, D, \mathbf{x}_k) = \sum_{j_k=1}^{m_k} p(Z_k, m_k, j_k | D, \mathbf{x}_k) \quad (2.36)$$

$$= \sum_{j_k=1}^{m_k} p(Z_k | m_k, j_k, D, \mathbf{x}_k) p(m_k | j_k, D, \mathbf{x}_k) p(j_k | D, \mathbf{x}_k) \quad (2.37)$$

$$= \frac{p_F(m_k - 1)}{m_k |\text{FoV}|^{m_k - 1}} \sum_{j_k=1}^{m_k} \mathcal{N}(\mathbf{z}_k^{j_k}; \mathbf{H}_k \mathbf{x}_k, \mathbf{R}_k^{j_k}). \quad (2.38)$$

Under the assumption j_k , we assume a Gaussian likelihood function for describing $\mathbf{z}_k^{j_k}$ according to Eq. 2.19, the other $m_k - 1$ measurements being treated as equally distributed in the sensor field of view:

$$p(Z_k | m_k, j_k, D, \mathbf{x}_k) = |\text{FoV}|^{-(m_k - 1)} \mathcal{N}(\mathbf{z}_k^{j_k}; \mathbf{H}_k \mathbf{x}_k, \mathbf{R}_k^{j_k}). \quad (2.39)$$

$p(m_k | j_k, D, \mathbf{x}_k)$ is given by $p_F(m_k - 1)$, while a priori the m_k data association hypotheses j_k are assumed to equally distributed, $p(j_k | D, \mathbf{x}_k) = m_k^{-1}$.

By exploiting the definition of the Poisson distribution and re-arranging the terms, a likelihood function for ambiguous data is proportional to a weighted sum of Gaussians and a constant ($\rho_F > 0$):

$$\ell(\mathbf{x}_k; Z_k, m_k) \propto (1 - P_D) \rho_F + P_D \sum_{j_k=0}^{m_k} \mathcal{N}(\mathbf{z}_{j_k}; \mathbf{H}_k \mathbf{x}_k, \mathbf{R}_k). \quad (2.40)$$

In the special case of $\rho_F = 0$ (no false measurements to be expected), Kronecker symbols can be used to find an expression for the likelihood ($\delta_{ij} = 1$ for $i = j$, $\delta_{ij} = 0$ otherwise):

$$\ell(\mathbf{x}_k; Z_k, m_k) \propto (1 - P_D) \delta_{0m_k} + P_D \mathcal{N}(\mathbf{z}_k; \mathbf{H}_k \mathbf{x}_k, \mathbf{R}_k) \delta_{1m_k}. \quad (2.41)$$

Possibly Irresolved Measurements

Similar considerations can be applied to formulate appropriate likelihood functions in multiple object situations described by joint object states $\mathbf{x}_k = (\mathbf{x}_k^{1\top}, \mathbf{x}_k^{2\top}, \dots)^\top$, where possibly irresolved measurements are to be taken into account (see Fig. 2.6b).

Among other sensor properties, in such situations the limited capability of physical sensors to resolve closely-spaced objects must be part of the sensor model. The link from physical resolution phenomena to the likelihood functions is provided by considering the probability P_u of two objects being irresolved. P_u certainly depends on the relative distance vector \mathbf{d}_k in proper coordinates between the objects at a certain time t_k : $P_u = P_u(\mathbf{d}_k)$. We qualitatively expect that P_u will be close to One for small values of $|\mathbf{d}_k|$, while $P_u = 0$ for distances significantly larger than certain resolution parameters, such as the beam-width, band-width, or coherence length of a radar. We expect a narrow transient region. In a generic model of the sensor resolution, we may describe P_u by a Gaussian-type function of \mathbf{d}_k with a ‘covariance matrix’ serving as a quantitative measure of the sensor resolution capability, which in particular reflects the extension and spatial orientation of ellipsoidal resolution cells depending on the underlying sensor-to-object geometry.

According to these considerations, the notion of a *resolution probability* is crucial if suitable sensor models for object groups are to be designed. The underlying Gaussian structure significantly simplifies the mathematical reasoning involved and finally leads to a representation of the likelihood function by a weighted sum of Gaussians and a constant, i.e. we have to deal with the same mathematical structure as before in the case of well-separated objects. For details see the discussion in Sect. 3.1.1.

2.3.4 Incorporating Signal Strength

The strength z_k of an received object signal at time t_k carries information on the corresponding object strength x_k , which is in a radar application, for example, directly

related to the object's characteristic mean radar cross section via the radar equation [23]. An individual sensor measurement related to an object state $X_k = (\mathbf{x}_k, x_k)$ is thus given by $Z_k^j = (\mathbf{z}_k^j, z_k^j)$. With this notation, the previous discussion can directly be generalized:

$$p(Z_k, m_k | X_k) = p(Z_k, m_k | \neg D, X_k) p(\neg D | X_k) + \sum_{j_k=1}^{m_k} p(Z_k | m_k, j_k, D, X_k) p(m_k | j_k, D, X_k) p(j_k | D, X_k). \quad (2.42)$$

We only have to consider the following conditional likelihood functions:

$$p(Z_k, m_k | \neg D, X_k) = |\text{FoV}|^{-m_k} \prod_{j=1}^{m_k} p(z_k^j | \neg D, X_k) =: \Lambda \quad (2.43)$$

$$p(Z_k | m_k, j_k, D, X_k) = \mathcal{N}(\mathbf{z}_k^{j_k}; \mathbf{H}_k \mathbf{x}_k, \frac{1}{z_k} \mathbf{R}_k^{j_k}) \frac{\Lambda p(z_k^{j_k} | D, X_k)}{|\text{FoV}|^{-1} p(z_k^{j_k} | \neg D, X_k)}. \quad (2.44)$$

We here additionally assumed a measurement error covariance matrix $\frac{1}{z_k} \mathbf{R}_k$ depending on the received signal strength z_k . This can be justified by radar signal processing theory [23] and reflects the empirical phenomenon that the weaker the signals received are the less accurate the resulting measurements.

For the sake of simplicity, we furthermore assume that $p(z_k | \neg D, X_k)$ and $p(z_k | D, X_k)$ do not depend on the kinematic state vector, although the received signal strength may in principle depend on the sensor-to-object geometry. The often highly complex dependency on the aspect angle is instead described by so-called Swerling models of radar cross section fluctuations [24]. According to the practically important Swerling-I-model, the received signal strengths z_k are random variables, characterized by $p(z_k | x_k) = e^{-z_k/(1+x_k)} / (1+x_k)$, i.e. simple exponential densities. Let us furthermore assume that a detector decides on “detection”, denoted by ‘D’, if z_k exceeds a certain threshold: $z_k > \lambda$. If there is actually an object present that has been detected, $P_D = p(\text{‘D’} | D)$ is thus given by:

$$P_D = \frac{1}{1+x_k} \int_{\lambda}^{\infty} dz_k e^{-z_k/(1+x_k)} = e^{-\lambda/(1+x_k)}. \quad (2.45)$$

The corresponding false alarm probability $P_F = p(\text{‘D’} | \neg D)$ is given by $P_F = \int_{\lambda}^{\infty} dz_k e^{-z_k} = e^{-\lambda}$. Here $x_k = 0$ is assumed for a noise-type target. This result directly leads to the famous *Swerling formula*, which relates the detection probability P_D to the object strength x_k and the false alarm probability P_F characterizing the detector:

$$P_D(x_k, P_F) = P_F^{\frac{1}{1+x_k}}. \quad (2.46)$$

A detected signal not belonging to a real object of interest is a clutter signal with a *clutter strength* c_k , a parameter characterizing context information on the sensing environment. After detection and according to Bayes Theorem, a received signal strength z_k is either distributed according to:

$$p(z_k | x_k, D) = \begin{cases} \frac{e^{(\lambda - z_k)/(1+x_k)}}{1+x_k} & \text{for } z_k > \lambda \\ 0 & \text{else} \end{cases} \quad (2.47)$$

or to:

$$p(z_k | x_k, -D) = \begin{cases} \frac{e^{(\lambda - z_k)/(1+c_k)}}{1+c_k} & \text{for } z_k > \lambda \\ 0 & \text{else.} \end{cases} \quad (2.48)$$

By inserting these densities in Eqs. 2.43 and 2.44, we directly obtain the modified likelihood function for ambiguous sensor data that include signal strength information:

$$\begin{aligned} \ell(\mathbf{x}_k, x_k; Z_k, m_k) &\propto (1 - e^{-\frac{\lambda}{1+x_k}}) \rho_F \\ &+ \sum_{j=1}^{m_k} \left(\frac{e^{(\lambda - z_k^j)/(1+c_k)}}{1+c_k} \right)^{-1} \frac{e^{-z_k^j/(1+x_k)}}{1+x_k} \mathcal{N}(\mathbf{z}_k^j; \mathbf{H}_k \mathbf{x}_k, \frac{1}{z_k^j} \mathbf{R}_k^j). \end{aligned} \quad (2.49)$$

Note that this likelihood function depends on the sensor parameters \mathbf{R}_k and λ , characterizing the measurement and the detection process, as well as the environmental parameters ρ_F and c_k . These parameters represent context information, which is a necessary input for the likelihood function besides the sensor data themselves.

2.3.5 Extended Object Likelihood

According to the discussion in Sect. 2.1, spatially extended objects or collectively moving object clusters, are characterized by an object state $X_k = (\mathbf{x}_k, \mathbf{X}_k)$, which consists of an kinematic state vector \mathbf{x}_k and a symmetric, positively definite matrix \mathbf{X}_k . For the sake of simplicity, let us exclude false or unwanted measurements at present. In a first approximation, the number m_k of measurements in Z_k is assumed to be independent of the object state X_k ,; i.e. $p(m_k | \mathbf{x}_k, \mathbf{X}_k)$ is assumed to be a constant.

In the case of extended or group targets, the significance of a single measurement is evidently dominated by the underlying object extension. The sensor-specific measurement error describing the precision by which a given scattering center is currently measured is the more unimportant, the larger the actual extension of the object is compared to the measurement error. The individual measurements must therefore rather be interpreted as measurements of the centroid of the extended or collective object, since it is unimportant, which of the varying scattering centers was actually responsible for the measurement.

We thus interpret each individual measurement produced by an extended object as a measurement of the object centroid with a corresponding ‘measurement error’ being proportional to the object extension \mathbf{X}_k to be estimated. By means of this ‘measurement error’, however, the object extension \mathbf{X}_k becomes explicitly part of the likelihood function $p(Z_k, m_k | \mathbf{x}_k, \mathbf{X}_k)$, which describes what the measured quantities Z_k, m_k can say about the state variables \mathbf{x}_k and \mathbf{X}_k . Elementary calculations, similar to those used in Sect. 2.3.2, yield the following factorization (see Appendix A.10 for details):

$$p(Z_k, m_k | \mathbf{x}_k, \mathbf{X}_k) \propto \prod_{j=1}^{m_k} \mathcal{N}(\mathbf{z}_k^j; \mathbf{H}_k \mathbf{x}_k, \mathbf{X}_k) \quad (2.50)$$

$$\propto \mathcal{N}(\mathbf{z}_k; \mathbf{H}_k \mathbf{x}_k, \frac{1}{m_k} \mathbf{X}_k) \mathcal{LW}(\mathbf{Z}_k; m_k - 1, \mathbf{X}_k) \quad (2.51)$$

up to a multiplicative constant independent of the state variables. In Eq. 2.51, the centroid measurement \mathbf{z}_k and the corresponding scattering matrix \mathbf{Z}_k are given by:

$$\mathbf{z}_k = \frac{1}{m_k} \sum_{j=1}^{m_k} \mathbf{z}_k^j \quad (2.52)$$

$$\mathbf{Z}_k = \sum_{j=1}^{m_k} (\mathbf{z}_k^j - \mathbf{z}_k)(\mathbf{z}_k^j - \mathbf{z}_k)^\top, \quad (2.53)$$

while $\mathcal{LW}(\mathbf{Z}_k; m_k - 1, \mathbf{X}_k)$ is proportional to a Wishart density with $m_k - 1$ degrees of freedom, a matrix-variate probability density function describing the properties of the random variable \mathbf{Z}_k (see Appendix A.11 for details):

$$\mathcal{LW}(\mathbf{Z}_k; m_k - 1, \mathbf{X}_k) = |\mathbf{X}_k|^{-\frac{m_k-1}{2}} \text{etr}\left(-\frac{1}{2}(\mathbf{Z}_k \mathbf{X}_k^{-1})\right). \quad (2.54)$$

References

1. R.R. Yager, L. Liu (eds.). *Classic works of the Dempster-Shafer theory of belief functions* (Springer, Berlin, 2008)
2. Y. Bar-Shalom, P.K. Willett, X. Tian, Tracking and Data Fusion. in *A Handbook of Algorithms* (YBS Publishing, Storrs, 2011)
3. X. Rong, Survey of maneuvering target tracking. Part I. dynamic models. *IEEE Trans. Aerosp. Electron. Syst.* **39**(4), 1333–1364 (2003)
4. X.R. Li, V.P. Jilkov, A survey of maneuvering target tracking-part II: ballistic target models. in *Proceedings of the 2001 SPIE Conference on Signal and Data Processing of Small Targets*, vol. 4473, 559–581 (2001)
5. X.R. Li, V.P. Jilkov, A survey of maneuvering target tracking-part III: measurement models, in *Proceedings of the 2001 SPIE Conference on Signal and Data Processing of Small Targets*, vol. 4473, pp. 423–446, 2001

6. X.R. Li and V.P. Jilkov, A survey of maneuvering target tracking-Part IV: decision-based methods. in *Proceedings of the 2002 SPIE Conference on Signal and Data Processing of Small Targets*, vol. 4728, p. 60, 2002
7. X. Rong, Li, V.P. Jilkov, Survey of maneuvering target tracking. Part V. Multiple model methods". in *IEEE Transactions on Aerospace and Electronic Systems* vol. 41(4) (2005), pp.1255–1321
8. G.V. Keuk, Zielverfolgung nach Kalman-anwendung auf elektronisches radar. FFM-Bericht, 173 (1971)
9. H.A.P. Blom. An efficient filter for abruptly changing systems. In *Proceedings of the 23rd IEEE Conference on Decision and Control*, Las Vegas, 1984
10. M. Michaelis, F. Govaers, W. Koch, State dependent mode transition probabilities, in IEEE ISIF Workshop Sensor Data Fusion-Trends, Solutions, Applications, Bonn, Germany (IEEE Xplore), October 2013
11. D. Robinson, W. Seels, Kalman-Filter, European Patent No. EP0452797B1, April 1992
12. R. Klemm, M. Mertens, Tracking of convoys by airborne STAP radar. In IEEE international conference on information fusion, Cologne, 2008
13. D.J. Torrieri, Statistical theory of passive location systems. *IEEE Trans. Aerosp. Electron. Syst.* **AES-20**(2), 183–198 (1984)
14. D. Musicki, R. Kaune, W. Koch, Mobile Emitter Geolocation and Tracking Using TDOA and FDOA Measurements. In *IEEE Transactions on Signal Processing* vol. 58(3) pp.1863–1874 (2010)
15. K. Becker, Three-dimensional target motion analysis using angle and frequency measurements. *IEEE Trans. Aerosp. Electron. Syst.* **41**(1), 284–301 (2005)
16. C.R. Berger, M. Daun, W. Koch. Low complexity track initialization from a small set of non-invertible measurements. *EURASIP J. Adv. Sig. Process.* special issue on track-before-detect techniques, 15, (756414) **2008** doi:[10.1155/2008/756414](https://doi.org/10.1155/2008/756414)
17. R. Baltes, A triangulation system for tracking multiple targets with passive sensors. in *Proceedings of the DGON/ITG International Radar Symposium IRS'98*, Muenchen, 1998
18. M. Daun, U. Nickel, W. Koch, Tracking in multistatic passive radar systems using DAB/DVB-T illumination. In *Proceedings of Signal Processing* pp 1365–1386 (2012)
19. W. Koch, Ground target tracking with STAP radar: selected tracking aspects. Chapter 15 in: R. Klemm (ed.), *The Applications of Space-Time Adaptive Processing*, (IEE Publishers, London, 2004)
20. W. Koch, M. Blanchette, Tracking in densely cluttered environment—concepts and experimental results. In *Proceedings of ISATA Robotics, Motion, and Machine Vision*, p.215 ff, Aachen, 1994
21. W. Koch, Experimental results on Bayesian MHT for maneuvering closely-spaced objects in a densely cluttered environment. In *IEE International Radar Conference RADAR'97*, Edinburgh, 729 (1999)
22. W. Koch, Generalized smoothing for multiple model/multiple hypothesis filtering: experimental results, in *Proceedings of European Control Conference ECC'99*, Karlsruhe, CD ROM 1999
23. W.-D. Wirth, *Radar Techniques Using Array Antennas*. (IEE Press, London, 2001)
24. P.L. Bogler, *Radar Principles with Applications to Tracking Systems* (Wiley, New York, 1990)

Tracking and Sensor Data Fusion

Methodological Framework and Selected Applications

Koch, W.

2014, XVII, 253 p. 79 illus., 6 illus. in color., Hardcover

ISBN: 978-3-642-39270-2